Laser and Particle Beams (2015), *33*, 641–646.
© Cambridge University Press, 2015 0263-0346/15
doi:10.1017/S0263034615000695

Stimulated compton scattering of surface plasma wave excited over metallic surface by a laser

DEEPIKA GOEL,[1] PRASHANT CHAUHAN,[1] ANSHU VARSHNEY,[1] D.B. SINGH,[2] AND VIVEK SAJAL[1]

[1]Department of Physics and Material Science & Engineering, Jaypee Institute of Information Technology, Uttar Pradesh, India
[2]Laser Science and Technology Center, Delhi, India

(RECEIVED 18 April 2015; ACCEPTED 16 June 2015)

Abstract

A high-frequency surface plasma wave (SPW) excited over metallic surface irradiated by a laser beam, can undergo stimulated Compton scattering if phase velocity of daughter plasma wave is equal to the Fermi velocity for metal. The pump SPW (ω_0, $\vec{k}_{0z}$) parametrically excites a quasi-electrostatic plasma wave (ω, $\vec{k}_z$) and a backscattered sideband SPW (ω_1, $\vec{k}_{1z}$) at resonance $\omega_0 = \omega - \omega_1$ and $\vec{k}_{0z} = \vec{k}_z - \vec{k}_{1z}$. The growth rate of Compton process increases with the frequency of incident laser and turns out to be 5.425×10^{10} rad/s at laser frequency $\omega_0 = 0.7595 \times 10^{15}$ rad/s for incident laser amplitude $A_{0L} = 11 \times 10^{11}$ V/m, laser spot size $b = 1.38 \times 10^{-5}$ m, and free electron density of metal $n_0 = 5.85 \times 10^{28}/\mathrm{m}^3$. The excitation of highly damped quasi-electrostatic plasma wave in this parametric process provide a better nonlinear option for surface heating as compared with direct laser heating. The process can also be used for diagnostics purposes.

Keywords: Parametric instability; Plasma-beam interactions; Surface plasma waves

1. INTRODUCTION

Nonlinear wave interactions and parametric instabilities in infinite plasmas have been studied extensively in the last decade because of its possible applications to laser fusion, plasma heating, and plasma current drive in fusion plasmas, as well as in space plasmas (Macchi *et al.*, 2002; Shoucri & Afeyan, 2010; Verma & Sharma, 2011; Singh & Sharma, 2013; Hao *et al.*, 2013; Vyas *et al.*, 2014). However such studies are rather few for bounded plasmas. Parametric decay of light wave into surface plasma wave (SPW) has been reported in literature because of its use for plasma diagnostics and for sustaining the plasma during plasma processing (Lee & Cho, 1999; Kumar & Tripathi, 2007). SPW can exist at the boundary separating two dielectric media with permittivities opposite in sign (Liu & Tripathi, 2000). The SPW can travel long distances along the interface and decays exponentially away from the interface in both media (decay is rapid in the conductor as compared with the dielectric). Hence the SPW field is localized in a thin skin layer. The properties of surface waves (SWs) propagating in bounded plasma structures are the subject of both experimental and theoretical studies. Their strong localization and resonant properties find application in solar cells and sensors etc., (Berndt *et al.*, 1991; Shin and Fan, 2006; Catchpole and Polman, 2008; Rani *et al.*, 2013). When an intense electromagnetic wave is incident on bounded plasma, these surface wave modes become coupled parametrically through the incident pump wave and decay instability of the SWs is expected to occur under suitable conditions (Aliev & Brodin, 1990; Brodin & Lundberg, 1991). The excitation of SPW by a laser pulse is not easily possible due to K-vector mismatch between the SPW and the laser. For a SPW propagating along the boundary of vacuum-metal interface (z-axis), the dispersion relation is given by $K_z^2 = (\omega_0^2/c^2)[\varepsilon\ /(1+\varepsilon\ )]$ where K_z is the wave vector of the SPW and ε is the dielectric constant of the metal (which is negative). The wave vector of the surface plasma wave is bigger than the wave vector of the electromagnetic wave in a vacuum. The K-vector mismatch can be overcome either by using the attenuated total reflection configuration or by creating a surface ripple of desired wave vector by a laser pulse (Kretschmann & Reather, 1968). Parashar *et al.* (1998) have developed a theory of the SPW excitation in the dense plasma via the stimulated

Address correspondence and reprint requests to: Vivek Sajal, Department of Physics and Material Science & Engineering, Jaypee Institute of Information Technology, Noida-201307, Uttar Pradesh, India. E-mail: vsajal@rediffmail.com

Compton scattering. Lee & Cho (1999) have developed theoretical model for the nonlinear decay of a light wave into two daughter surface plasma waves. Shin *et al.* (2007) introduced the sub wavelength transmission of an effective surface plasmon beyond the light zone via the proximity interaction of convection electrons with a metal grating. Singh and Tripathi (2007) gave a theoretical model to excite surface plasma wave at frequency $\omega = \omega_1 - \omega_2$ by beating of two coplanar laser beams of frequencies ω_1 and ω_2 impinged on a metal surface. The lasers exert a ponderomotive force on electrons in the skin layer and drive the SPW. The SPW heats the electrons efficiently, causing efficient ablation of the material. Kumar and Tripathi (2007) suggested that the parametric decay of a light wave into pair of counter propagating SPWs at the vacuum–plasma interface is possible due to the plasma density perturbation at $2\omega_0$ frequency associated with the ponderomotive force of the laser pulse on the plasma surface. The growth rate of the parametric process is the maximum for normal incidence of the laser pulse and it decreases with the angle of incidence. Recently, Tinakiche *et al.* (2012) investigated three-wave coupling process in electron–positron-ion plasmas interacting with an electromagnetic pump wave.

In this paper, we have studied the stimulated Compton scattering of a surface plasma wave propagating on vacuum–metal interface. The SPW can be excited at the interface by a high-frequency laser (Liu & Tripathi, 2000). The SPW $(\omega_0, \vec{k}_{0z})$ acts as a pump and resonantly excites a quasi-electrostatic plasma mode along with a sideband SPW having frequency $\omega_1 = \omega - \omega_0$ and wave number $\vec{k}_{1z} = \vec{k}_z - \vec{k}_{0z}$. The density perturbation due to plasma wave couples with the oscillatory velocity of metal electrons (due to pump wave) and produce nonlinear current density ($\vec{J}_1^{\mathrm{NL}}$) driving the sideband SPW. The sideband wave couples nonlinearly with pump wave to exert a nonlinear ponderomotive force on metal electrons at the beat frequencies ($\omega_0 = \omega - \omega_1$) driving the quasi-plasma mode having phase velocity equal to fermi velocity. The excited quasi-electrostatic fields can be utilized for heating plasma along with SPW by anomalous wave energy absorption mechanism. Growth rate equation is obtained on the basis of parametric coupling of a pump SPW, a plasma wave and a sideband SPW. Parametric coupling and conclusions are given in section II and III, respectively.

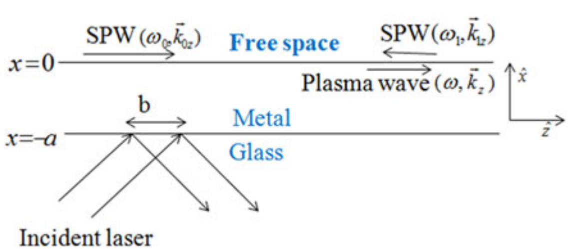

Fig. 1. Schematic of surface plasma wave Compton scattering at the vacuum–metal interface.

2. PARAMETRIC COUPLING

Consider the multilayered structure of glass ($x < -a$), metal ($x < 0$), and free space ($x > 0$). A laser is obliquely incident from the glass side on the glass–metal interface having field, given by (Liu & Tripathi, 2000)

$$\vec{E}_1 \cong \vec{A}_{0L} e^{[-\{(x+a)\sin\theta_i - z\cos\theta_i\}^2/b'^2]} e^{-i(\omega_0 t - \vec{k}_0 . \vec{r})} \tag{1}$$

where 'a' is the width of the metal, θ_i is the angle of incidence and $b' = b\cos\theta_i$ and b is the spot size of laser. The incident laser excites a SPW on metal free space interface ($x = 0$) propagating along z-direction (as shown in Fig. 1). The electric field profile of the SPW $(\omega_0, \vec{k}_{0z}; \vec{k}_0 = \vec{k}_{0z}\hat{z} - i\alpha_0\hat{x})$ is given by

$$\vec{E}_0 = \vec{A}_{0z}(x) e^{-i(\omega_0 t - k_{0z}\hat{z})} \tag{2}$$

where $A_{0z} = A_{0s}\left(\hat{z} - \frac{ik_{0z}}{\alpha_0}\hat{x}\right)e^{\alpha_0 x}$ ($x < 0$, metal)

$A_{0z} = A_{0s}\left(\hat{z} + \frac{ik_{0z}}{\alpha_0'\hat{x}}\right)e^{-\alpha_0' x}$ ($x > 0$, vacuum)

The amplitude of the wave for the free space at $x = 0$ and $z = 0$ is given by

$$A_{0s} = \frac{A_{0L} b}{2\sqrt{\pi}} T_{00}(\sigma_1 + i\sigma_2) I \tag{3}$$

where $T_{00} = (2i\psi_1 e^{\alpha_0 a})/(1 + i\psi_1)$

$$\psi_1 = \frac{\eta_g}{\left|1 + \varepsilon'_0(1 - 1/\eta_g^2)\right|^{1/2}}$$

$$\psi_2 = \frac{2(1 + i\psi_1)\omega_0|\varepsilon'_0|^{3/2}}{(1 - i\psi_1)c|1 + \varepsilon'_0|^{1/2}({\varepsilon'_0}^2 - 1)}$$

$$I = \int_{-\infty}^{\infty} \frac{e^{-p^2}(p - \sigma_1 b/2 + i\sigma_2 b/2)}{((p - \sigma_1 b/2)^2 + (\sigma_2 b/2)^2)} \mathrm{d}p$$

In the above expression $\eta_g = 1.5$, $\psi_2 \exp(-2\alpha_0 a) = \sigma_1 + i\sigma_2$, $\alpha_0^2 = k_{0z}^2 - (\omega_0^2/c^2)\varepsilon_0'$ and ${\alpha_0'}^2 = k_{0z}^2 - (\omega_0^2/c^2)$. The dielectric constant of the metal at frequency ω_0 is given by $\varepsilon_0' = \varepsilon_l - \omega_p^2/\omega_0^2$. ε_l and $\omega_p = \sqrt{n_0 e^2/m\varepsilon}$ are the lattice permittivity of metal and plasma frequency, respectively, $\varepsilon = 8.854 \times 10^{-12}$ f/m, $n_0 = 5.85 \times 10^{28}/m^3$ for silver metal; $-e$ and m is the charge and effective mass of electron, respectively. On applying conditions of continuity $\varepsilon_0' E_{0x}$ and E_{0z} at $x = 0$ along x and z directions, the dispersion relation of the SPW is given by

$$k_{0z} = \frac{\omega_0}{c}\sqrt{\frac{\varepsilon'_0}{1 + \varepsilon'_0}} \tag{4}$$

The pump SPW imparts oscillatory velocity to electrons ($\vec{v}_0 = e\vec{E}_0/mi\omega_0$). At resonance, the pump SPW decay into a quasi-electrostatic plasma wave (ω, $\vec{k}_z$) of potential (ϕ),

$$\phi = A(x)e^{-i(\omega t - k_z \hat{z})} \tag{5}$$

and a sideband SPW ($\omega_1, \vec{k}_{1z}; \vec{k}_1 = k_{1z}\hat{z} - i\alpha_1\hat{x}$) of electric field ($\vec{E}_1$)

$$\vec{E}_1 = \vec{A}_{1z}(x)e^{-i(\omega_1 t - k_{1z}\hat{z})} \tag{6}$$

where $A_{1z} = A_1\left(\hat{z} - \dfrac{ik_{1z}}{\alpha_1}\hat{x}\right)e^{\alpha 1x}$ ($x < 0$, metal)

$A_{1z} = A_1\left(\hat{z} + \dfrac{ik_{1z}}{\alpha'_1}\hat{x}\right)e^{-\alpha 1x}$ ($x > 0$, vacuum)

where $\alpha_1^2 = k_{1z}^2 - (\omega_1^2/c^2)\varepsilon_1$ and $\alpha_1'^2 = k_{1z}^2 - (\omega_1^2/c^2)$. The dielectric constant of sideband SPW at frequency ω_1 is $\varepsilon_1 = \varepsilon_l - \omega_p^2/\omega_1^2$. The phase matching conditions for parametric decay are $\vec{k}_z = \vec{k}_{0z} + \vec{k}_{1z}$ and $\omega = \omega_0 + \omega_1$. The sideband SPW imparts oscillatory velocity to electrons ($\vec{v}_1 = e\vec{E}_1/mi\omega_1$) and couples nonlinearly with the pump wave to exert a ponderomotive force on electrons at frequency ω, which is given by

$$\vec{F}_p = -m[\vec{v}.\nabla\vec{v}] - e[\vec{v}\times\vec{B}] \tag{7}$$

Replace $\vec{v}$ by $\vec{v}_0 + \vec{v}_1$ and $\vec{B}$ by $\vec{B}_0 + \vec{B}_1$ in the above equation, where $\vec{B}_0 = i\vec{k}_0 \times \vec{E}_0/i\omega_0$ and $\vec{B}_1 = i\vec{k}_1 \times \vec{E}_1/i\omega_1$ for pump and sideband SPW, respectively. On substituting these values into Eq. (7), we obtained

$$\vec{F}_p = e\nabla\Phi_p \tag{8}$$

where $\Phi_p = A_{0s}(x)\, A_1(x)\left(\dfrac{e}{2m\omega_0\omega_1}\right)\left(1 - \dfrac{k_{0z}k_{1z}}{\alpha_0\alpha_1}\right)e^{-i(\omega t - k_z z)}$, termed as ponderomotive potential.

This ponderomotive force along with self-consistent low-frequency field on the metal free electrons drive plasma oscillations at frequency ω. Hence, the equation of motion of electron becomes

$$m\frac{\partial\vec{v}_\omega}{\partial t} = e\nabla(\phi + \Phi_p) - m\upsilon\,\vec{v}_\omega$$

where υ is the collision frequency. Here, the collisions are considered effective only for low-frequency plasma wave for which phase velocity is close to the Fermi velocity of free electrons. For high-frequency SPWs collisional effects are neglected. The oscillatory velocity ($\vec{v}_\omega$) of electron at frequency (ω) is obtained by solving above equation of motion, given by

$$\vec{v}_\omega = -\frac{e\left[-i\nabla\Phi_p - i\dfrac{\partial\phi}{\partial x}\hat{x} + k_z\phi\,\hat{z}\right]}{m(\omega + i\upsilon)} \tag{9}$$

Substituting the value of oscillatory velocity from Eq. (9) into continuity equation ($\partial n/\partial t + \nabla\cdot(n_0\vec{v}_\omega) = 0$), we obtain the density perturbation (n) due to oscillatory motion of metal electrons.

$$n = \frac{\chi_e}{4\pi e}\left[-\nabla^2\Phi_p - \left(\frac{\partial^2\phi}{\partial x^2} - k_z^2\phi\right)\right] \tag{10}$$

where $\chi_e = -\omega_p^2/\omega\ (\omega + i\upsilon)$.

n_0 is the electron density inside the metal. Using n in Poisson's equation, we get

$$\nabla^2\phi = \frac{-\chi_e}{(\varepsilon_l + \chi_e)}\left[-k_z^2 + (\alpha_0 + \alpha_1)^2\right]\Phi_p$$

The density perturbations couples with oscillatory movement of metal electrons at frequency ω_0 (due to pump SPW) and excites a nonlinear current density ($\vec{J}_1^{NL}$) at the sideband frequency ω_1, which is given by

$$\vec{J}_1^{NL} = \frac{1}{2}env_0^* \tag{11}$$

On substituting values of n and v_0^* ($v_0^* = -e\vec{E}_0/mi\omega_0$, oscillatory velocity of electrons at frequency ω_0), the nonlinear current density is given by

$$\vec{J}_1^{NL} = \frac{ie\chi_e}{8\pi m\omega_0}\left(\frac{\varepsilon_l}{\varepsilon_l + \chi_e}\right)\nabla^2\Phi_p\vec{E}_0^* \tag{12}$$

This nonlinear current density ($\vec{J}_1^{NL}$) is responsible for the growth of sideband SPW whose characteristic equation can be derived by solving wave equation. The wave equation governing electric field of SPW at the sideband frequency can be written as

$$\nabla^2\vec{E}_1 - \nabla(\nabla\cdot\vec{E}_1) = \frac{4\pi}{c^2}\frac{\partial\vec{J}_1^{NL}}{\partial t} + \frac{\varepsilon_l}{c^2}\frac{\partial^2\vec{E}_1}{\partial t^2} \tag{13}$$

Taking the divergence of the Eq. (13), we obtain

$$\nabla\cdot\vec{E}_1 = \frac{4\pi i}{\omega_1\varepsilon_1}\nabla\cdot\vec{J}_1^{NL} \tag{14}$$

Substituting Eq. (14) into Eq. (13), we obtain

$$\nabla^2\vec{E}_1 - \frac{\varepsilon_l}{c^2}\frac{\partial^2\vec{E}_1}{\partial t^2} = \frac{4\pi}{c^2}\frac{\partial\vec{J}_1^{NL}}{\partial t} + \frac{4\pi}{i\omega_1\varepsilon_1}\nabla(\nabla\cdot\vec{J}_1^{NL}) \tag{15}$$

After the Fourier analysis of Eq. (15), we have

$$\frac{\omega_1^2 - \omega_{1r}^2}{c^2}\varepsilon_1\vec{E}_1 = \frac{4\pi i\omega_1}{c^2}\vec{J}_1^{NL}\frac{4\pi i\omega_1}{\omega_1^2\varepsilon_1}\nabla(\nabla\cdot\vec{J}_1^{NL}) \tag{16}$$

Taking the dot product of Eq. (16) with $\vec{E}_1^*$ and integrating

https://doi.org/10.1017/S0263034615000695 Published online by Cambridge University Press

from $-\infty$ to ∞ with respect to x, we have

$$\frac{\omega_1^2-\omega_{1\mathrm{r}}^2}{c^2}\left[\int_{-\infty}^{0}\varepsilon_1\vec{E}_1\cdot\vec{E}_1^*\mathrm{d}x+\int_{0}^{\infty}\vec{E}_1\cdot\vec{E}_1^*\mathrm{d}x\right] = -\frac{4\pi i\omega_1}{c^2}\int_{-\infty}^{0}\vec{J}_1^{\mathrm{NL}}\cdot\vec{E}_1^*\mathrm{d}x-\frac{4\pi i\omega_1}{\omega_1^2\varepsilon_1}\int_{-\infty}^{0}\nabla(\nabla\cdot\vec{J}_1^{\mathrm{NL}})\cdot\vec{E}_1^*\mathrm{d}x \tag{17}$$

Here, $\varepsilon_1=\varepsilon_l-\omega_p^2/\omega_1^2$ for metal $(x<0)$ and $\varepsilon_1=1$ for vacuum $(x>0)$. Further, substituting the value of nonlinear current from Eq. (12). Then Eq. (17)

$$\omega_1^2-\omega_{1\mathrm{r}}^2=-\frac{e^2k^2\chi_e}{4m^2\omega_0^2\omega_1^2\varepsilon_1}\left(\frac{\varepsilon_l}{\varepsilon_l+\chi_e}\right)\left(1-\frac{k_{0z}k_{1z}}{\alpha_0\alpha_1}\right)\left(\frac{\alpha_1\alpha'_1}{\alpha_0+\alpha_1}\right)\frac{\left[\omega_1^2\varepsilon_1-c^2k_{1z}^2+c^2(2\alpha_0+\alpha_1)^2\right]}{(\varepsilon_1\alpha'_1-\alpha_1)}|E_0|^2 \tag{18}$$

where $\chi_e=-\omega_p^2/\omega\,(\omega+i\upsilon)$, $k_{0z}=\omega_0/c\sqrt{\varepsilon'_0/1+\varepsilon'_0}$, $k_{1z}=\omega_1/c\sqrt{\varepsilon_1/1+\varepsilon_1}$, $\alpha_0^2=k_{0z}^2-(\omega_0^2/c^2)\varepsilon_0'$, $\alpha_1^2=k_{1z}^2-(\omega_1^2/c^2)\varepsilon_1$ and $\alpha_1'^2=k_{1z}^2-(\omega_1^2/c^2)$. Eq. (18) is the dispersion relation for Compton process. Growth rate (γ) for the process can be deduced by solving Eq. (18) that comes out as follows:

$$\gamma=-\frac{e^2k^2\varepsilon_l^2\omega\upsilon}{8m^2\omega_0^2\omega_p^2(\omega-\omega_0)^3}\left(1-\frac{k_{0z}k_{1z}}{\alpha_0\alpha_1}\right)\left(\frac{\alpha_1\alpha'_1}{\alpha_0+\alpha_1}\right)\left(\frac{(\omega-\omega_0)^2\varepsilon_1-c^2k_{1z}^2+c^2(2\alpha_0+\alpha_1)^2}{(\varepsilon_1\alpha'_1-\alpha_1)}\right)|E_0|^2 \tag{19}$$

where $\omega_1=\omega_{1\mathrm{r}}+i\gamma$ and $k^2=(\alpha_0+\alpha_1)^2-(k_{0z}+k_{1z})^2$.

Eq. (19) is normalized and numerically solved using the parameters $\varepsilon_l=4$, $T_e=63600$ K (Fermi temperature for silver) and $\omega_p=2.17\times10^{15}$ rad/s. The growth rate of Compton process increases with the frequency of incident laser and turns out to be $2.5\times10^{-5}\,\omega_p$ at laser frequency $\omega_0=0.35\omega_p$ for incident laser amplitude $A_{0L}=0.3\,m\omega_pc/e$, laser spot size $b=100c/\omega_p$. Here, width of the metal is $(a\omega_0/c)=0.5$ and free electron density of silver metal is $n_0=5.85\times10^{28}/\mathrm{m}^3$. The frequency of quasi-static plasma mode can be calculated from the resonance condition $\vec{k}_{0z}=\vec{k}_z-\vec{k}_{1z}$ where $\vec{k}_z=\omega/v_F$. Here, v_F is the Fermi velocity of electrons for silver. Figure 2 depicts the variation of plasma mode frequency (ω/ω_p) with pump frequency (ω/ω_p). Here, plasma frequency increases linearly with frequency of pump wave. This is due to the fact that with increase in pump frequency, there is corresponding increase in its wave number. Hence, to satisfy the resonance conditions, there should be a related increase in the plasma mode frequency. Amplitude of SPW $(eA_{0S}/m\omega_pc)$ is plotted as a function of incident laser spot size $(b\omega_p/c)$ on varying width of the metal film $(b\omega_0/c)$ and amplitude of laser $(eA_{0L}/m\omega_pc)$ in Figures 3a and 3b, respectively. Figure 3a shows that for smaller values of spot size, the amplitude of SPW increases linearly and saturates at higher values of $b\omega_p/c$. From Eq. (3), the amplitude of SPW is larger than the laser amplitude for the condition $b\omega_p/c>\exp(a\omega_0/c)$, where b and a are the spot size of laser and the width of the metal, respectively (Liu & Tripathi, 2000). On increasing b and keeping a fixed, the inequality

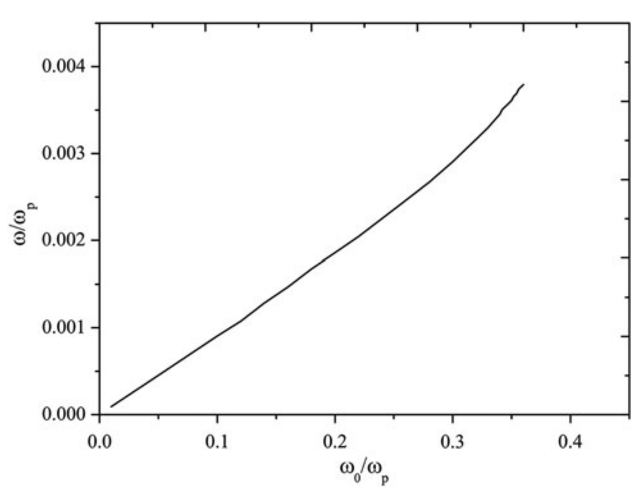

Fig. 2. Variation of normalized plasma wave frequency (ω/ω_p) with normalized pump wave frequency (ω_0/ω_p).

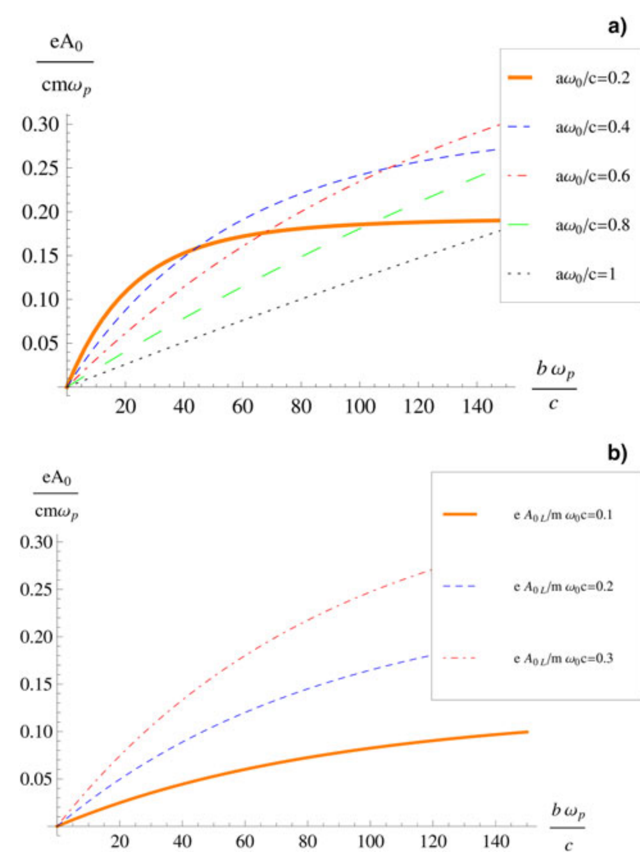

Fig. 3. Plot of surface plasma wave amplitude versus laser spot size $(b\omega_p/c)$ on varying (a) width of the metal layer $(b\omega_0/c)$ for $(eA_{0L}/m\omega_pc)=0.3$ and (b) laser amplitude $(eA_{0L}/m\omega_pc)$ for $(a\omega_0/c)=0.5$.

https://doi.org/10.1017/S0263034615000695 Published online by Cambridge University Press

grows, resulting in increased amplitude of the SPW as observed in Figure 3a. The saturation value of amplitude is larger for metal films of larger width and it occurs at larger spot size of the laser. For $(a\omega_0/c = 0.5)$, the amplitude of SPW further increases with the laser amplitude as observed in Figure 3b. As the laser intensity increases, evanescent wave provides higher oscillatory velocity to the electrons and couple with the pump wave to exert ponderomotive on electron at $(\omega, \vec{k}_z)$ and excites the SPW of higher amplitude. Enhanced amplitude of SPW at metal free space interface is reported by Raether (1988) and Liu and Tripathi, (1998).

Figure 4 shows the variation of SPW amplitude with pump frequency and width of the metal. Other parameters are $(eA_{0L}/m\omega_p c) = 0.3$ and $(b\omega_p/c) = 100$. As the metal thickness increases, the evanescent field has to penetrate longer distances to excite the SPW. Also, the condition $[b\omega_0/c > \exp(a\omega_0/c)]$ approaches towards equality on increasing *a*, resulting in decrease of SPW amplitude with the metal width as observed in Figure 4. In Figures 5a and 5b, growth rate (γ/ω_p) of the Compton process is plotted as a function of pump frequency for various combinations of laser spot size and its amplitude for $(a\omega_0/c) = 0.5$. The growth rate of the Compton process increases with the pump frequency because SPW is strongly localized near the interface and propagates along the interface with low attenuation. Increased amplitude of the SPW at the metal free space interface as observed in Figures 3a and 3b enhances the ponderomotive force [Eq. (8)] on electrons. As a result, the growth rate increases with incident laser spot size and its amplitude as shown in Figures 5a and 5b, respectively. Lee and Cho (1999) theoretically investigated the decay of high-frequency light wave into two daughter SWs and reported the increase in growth rate of the surface wave with the light wave frequency. Drake *et al.* (1990) have experimentally studied the stimulated Compton scattering on electrons from laser produced plasma and reported that stimulated Compton scattering increases with the laser intensity. Variation of growth rate of the Compton process with width of the metal is plotted in Figure 6. Other parameters are same as Figure 4. Increased width of the metal surface leads to lesser amplitude of SPW at the metal free space interface and lesser ponderomotive force on electrons to drive the quasi-static plasma mode, resulting in decrease of growth rate with the metal width.

3. CONCLUSIONS

In this work, we discussed Compton scattering of SPW propagating at the metal–vacuum interface. This wave can be excited by a high-frequency laser. The parametric decay of SPW into another SPW can be realized via quasi-static plasma wave in metals. The quasi-static plasma wave is damped (as its phase velocity is equal to the Fermi velocity (v_F) of the metal), by the free electrons, resulting into surface heating. Growth rate of the Compton process increases with the pump wave frequency, width of the metal layer, laser amplitude, and its spot size. It increases threefold as the

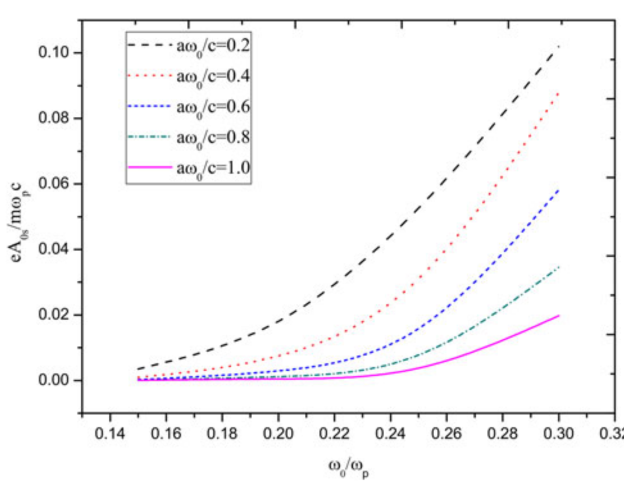

Fig. 4. Plot of surface plasma wave amplitude versus pump frequency and width of metal. The other parameters are $(eA_{0L}/m\omega_p c) = 0.3$ and $(b\omega_p/c) = 100$.

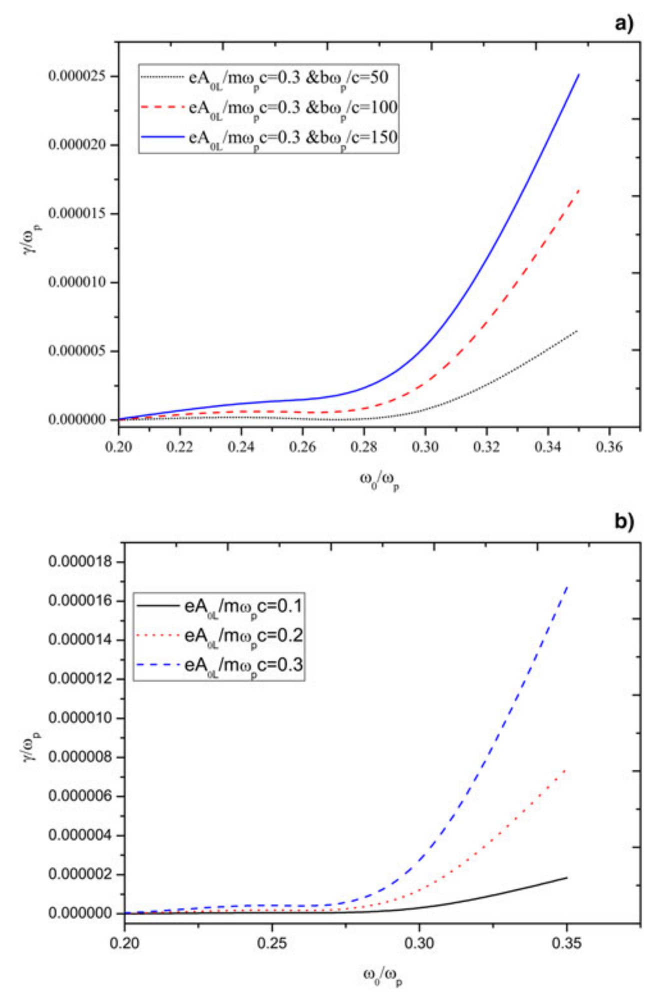

Fig. 5. Plot of growth rate (γ/ω_p) of the Compton process versus pump frequency on varying (a) spot size of laser for $(eA_{0L}/m\omega_p c) = 0.3$ and (b) its amplitude for $(b\omega_p/c) = 100$ at $(a\omega_0/c) = 0.5$.

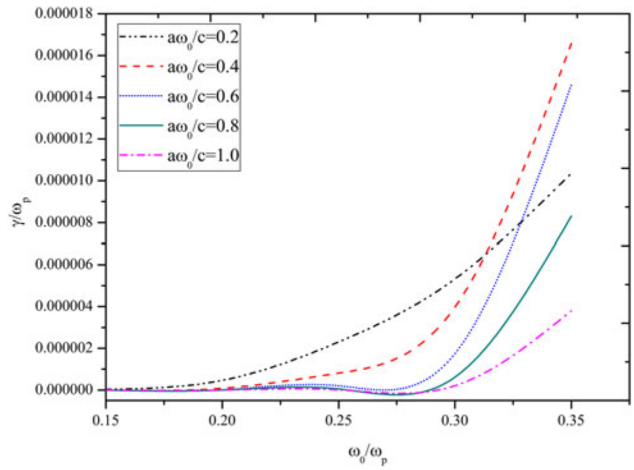

Fig. 6. Variation of growth rate of the Compton process versus pump frequency on varying width of the metal. The other parameters are $(eA_{0L}/m\omega_p c) = 0.3$ & $(b\omega_p/c) = 100$.

frequency increases from 0.25 to $0.35\omega_p$. However, growth rate of Compton process is found to decrease with the width of metal layer for higher values of pump frequency. As this process is sensitive to pump frequency variation, one can suitably choose among available lasers for material processing. The Compton process can produce energetic electrons travelling along the plasma boundary. These electrons in turn can give rise to stronger X-ray emission which can be utilized for various purposes along with the plasma diagnostics (Shivarova *et al*., 1975; Zhaoquan, *et al*., 2012).

REFERENCES

Aliev, Yu.M. & Brodin, G. (1990). Instability of strongly inhomogeneous plasma. *Phys. Rev. A* **42**, 2374.

Berndt, R., Gimzewski, J.K. & Johansson, P. (1991). Inelastic tunneling excitation of tip-induced plasmon modes on noble-metal surfaces. *Phys. Rev. Lett*. **67**, 3796.

Brodin, G. & Lundberg, J. (1991). Parametric excitation of surface waves in a strongly inhomogeneous plasma. *J. Plasma Phys*. **46**, 299–307.

Catchpole, K.R. & Polman, A. (2008). Plasmonic solar cells. *Opt. Express* **16**, 21793–21800.

Drake, R.P., Baldis, R.L., Kruer, W.L., Williams, E.A., Estabrook, K., Johnston, T.W. & Young, P.E. (1990). Observation of stimulated Compton scattering from resonant electrons in a laser produced plasma. *Phys. Rev. Lett*. **64**, 1990.

Raether, H. (1988). Surface plasmons on smooth and rouge surfaces and on gratings. New York: Springer-Verlag.

Hao, L., Liu, Z.J., Hu, X.Y. & Zheng, C.Y. (2013). Competition between the stimulated Raman and Brillouin scattering under the strong damping condition. *Laser Part. Beams* **31**, 203–209.

Kretschmann, E. & Reather, H. (1968). Radiative decay of non radiative surface plasmons excited by light. *Z. Naturforschung* **23a**, 2135–2136.

Kumar, N. & Tripathi, V.K. (2007). Parametric excitation of surface plasma waves in an overdense plasma irradiated by an ultrashort laser pluse. *Phys. Plasma* **14**, 103108.

Lee, H.J. & Cho, S.H. (1999). Parametric coupling of light wave and surface plasma waves. *Phys. Rev. E* **59**, 3503–3511.

Liu, C.S. & Tripathi, V.K. (1998). Diffraction-limited laser excitation of a surface plasma wave and its scattering on a rippled metallic surface. *IEEE J. Quantum Electron*. **34**, 1503.

Liu, C.S. & Tripathi, V.K. (2000). Excitation of surface plasma waves over metallic surfaces by lasers and electron beams. *IEEE Trans. Plasma Sci*. **28**, 2.

Macchi, A., Battaglini, M., Cornolti, F., Lisseikina, T.V., Pegoraro, F., Ruhl, H. & Vshivkov, V.A. (2002). Parametric generation of surface deformations in laser interaction with overdense plasmas. *Laser Part. Beams* **20**, 337–340.

Prashar, J., Pandey, H.D. & Tripathi, V.K. (1998). Laser excitation of surface waves over a dense plasma. *J. Plasma Phys*. **59**, 97–102.

Rani, M., Sharma, N.K. & Sajal, V. (2013). Localized surface plasmon resonance based fiber optic sensor with nanoparticles. *Opt. Commun*. **292**, 92–100.

Shin, H. & Fan, S. (2006). All angle negative refraction for surface plasmon waves using a metal-dielectric-metal structure. *Phys. Rev. Lett*. **96**, 073907.

Shivarova, A., Stoychev, T. & Russeva, S. (1975). Surface wave propagation along a current carrying warm plasma. *J. Phys. D: Appl. Phys*. **8**, 383.

Shoucri, M. & Afeyan, B. (2010). Studies of the interaction of an intense laser beam normally incident on an overdense plasma. *Laser Part. Beams* **28**, 129–147.

Singh, D.B. & Tripathi, V.K. (2007). Laser beat wave excitation of surface plasma wave and material ablation. *Phys. Plasma* **14**, 103115.

Singh, R.K. & Sharma, R.P. (2013). Stimulated Raman backscattering of filamented hollow Gaussian beams. *Laser Part. Beams* **31**, 387–394.

Shin, Y.M., So, J.K., Jang, K.H., Won, J.H., Srivastava, A. & Park, G.S. (2007). Evanescent tunnelling of an effective surface plasmon excited by convection electrons. *Phys. Rev. Lett*. **99**, 147402.

Tinakiche, N., Annou, R. & Tripathi, V.K. (2012). Three-wave coupling in electron-positron-ion plasmas. *Phys. Plasmas* **19**, 072114.

Verma, U. & Sharma, A.K. (2011). Nonlinear electromagnetic Eigen modes of a self created magnetized plasma channel and its stimulated Raman scattering. *Laser Part. Beams* **29**, 471–477.

Vyas, A., Singh, R.K. & Sharma, R.P. (2014). Study of coexisting stimulated Raman and Brillouin scattering at relativistic laser power. *Laser Part. Beams* **32**, 657–663.

Zhaoquan, C., Guangqing, X., Minghai, L., Yelin, H., Xiaoliang, Z., Ping, L., Qiyan, Z. & Xiwei, H. (2012). Character diagnosis for surface-wave plasmas excited by surface plasmon polaritons. *Plasma Sci. Technol*. **14**, 8.